

α -Fe₂O₃/TiO₂ 3D Hierarchical Nanostructures for enhanced Photoelectrochemical Water Splitting

Hyungkyu Han¹, Francesca Riboni², Frantisek Karlicky^{1,3}, Stepan Kment¹, Anandarup Goswami¹, P. Sudhagar⁴, Jeongeun Yoo², Lei Wang², Ondrej Tomanec¹, Martin Petr¹, Ondrej Haderka¹, Chiaki Terashima⁴, Akira Fujishima⁴, Patrik Schmuki^{2,5*} and Radek Zboril^{1*}

¹ Regional Centre of Advanced Technologies and Materials, Department of Physical Chemistry, Faculty of Science, Palacky University, Slechtitelu 11, 783 71 Olomouc, Czech Republic

² Department of Materials Science and Engineering, University of Erlangen-Nuremberg, Martensstrasse 7, D-91058 Erlangen, Germany

³ Department of Physics, Faculty of Science, University of Ostrava, 30. dubna 22, 701 03 Ostrava, Czech Republic

⁴ Photocatalysis International Research Center, Research Institute for Science and Technology, Tokyo University of Science, 2641 Yamazaki, Noda, Chiba 278-8510, Japan

⁵ Department of Chemistry, Faculty of Science, King Abdulaziz University, P.O. Box 80203, Jeddah 21569, Saudi Arabia

*Corresponding authors. Patrik Schmuki (E-mail: schmuki@ww.uni-erlangen.de), Radek Zboril (E-mail: radek.zboril@upol.cz)

S1. Theoretical simulation

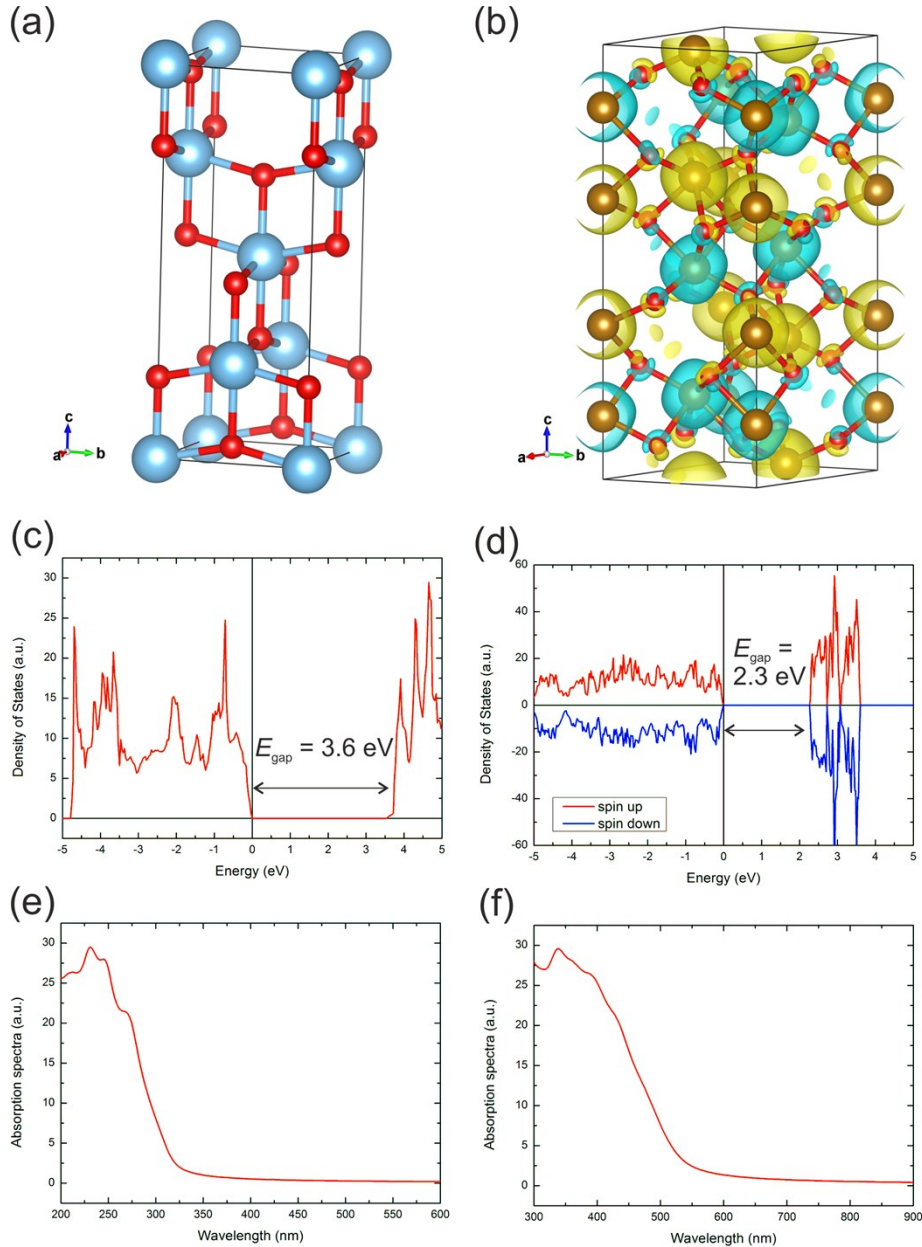


Figure S1. Calibration of the computational setup. (a-b) Atomic structure of the unit cell (Ti – blue, Fe – gold, O - red) and spin density surface (blue and yellow for up and down spin, respectively) for isovalue of 0.01 a.u., (c-d) density of electronic states and (e-f) optical spectra of bulk anatase TiO₂ (left column) and bulk hematite α -Fe₂O₃ (right column) calculated by PBE+U DFT. The choice of $U = 7.5$ eV for Ti atoms and $U = 4.3$ eV for Fe atoms provides fine agreement with literature data: $E_{\text{gap}} \sim 3.6$ eV of TiO₂ is close to experimental value (electronic band gap unknown, indirect optical gap of 3.2 eV¹) and reproduces calculated benchmark G_0W_0 electronic band gap of 3.7 eV². Magnetic moment $\mu \approx 4.2 \mu_B$ on Fe in antiferromagnetic α -Fe₂O₃ is close to experimental value of 4.9 μ_B ; $E_{\text{gap}} \sim 2.3$ eV is close to experimental value (2.2 eV³, 2.0-2.7 eV⁴).

¹ J. Am. Chem. Soc. 118 (1996) 6716; ² J. Phys.-Condens. Mater. 24 (2012) 202201; ³ J. Solid State Chem. 27 (1979) 307; ⁴ Phys. Rev. B 34 (1986) 7318

S2. Surface morphology results

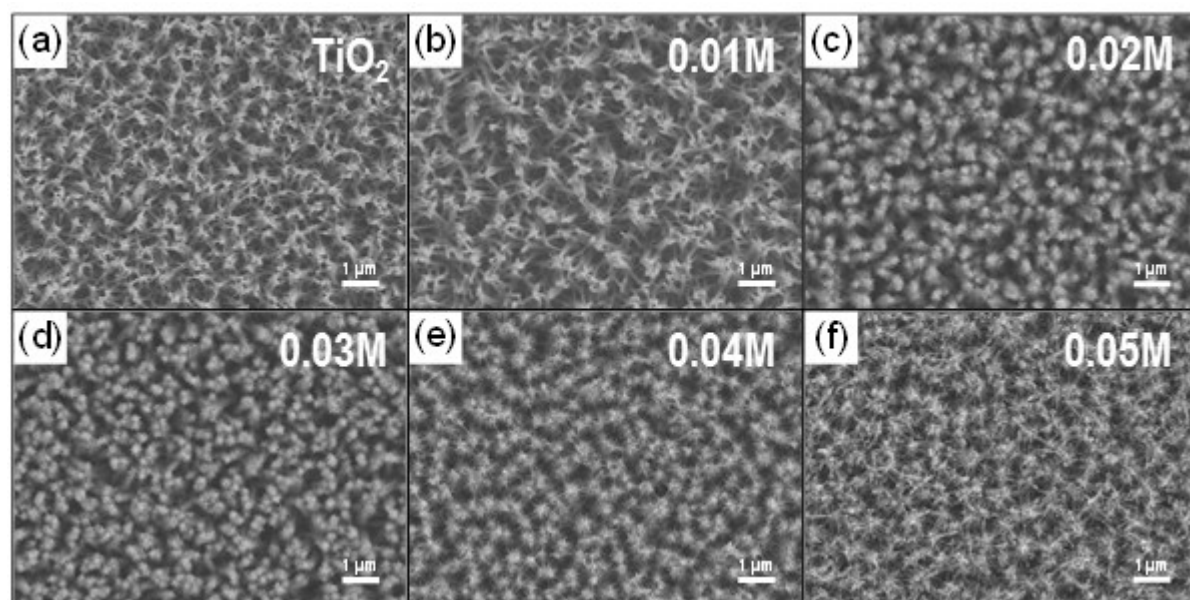


Figure S2. Top view SEM images of (a) TiO₂ NTs and (b–f) α -Fe₂O₃/TiO₂ NT composites prepared starting from Fe(III) precursor solutions with different concentrations (*i.e.*, 0.01–0.05 M).

S3. Cross section SEM results

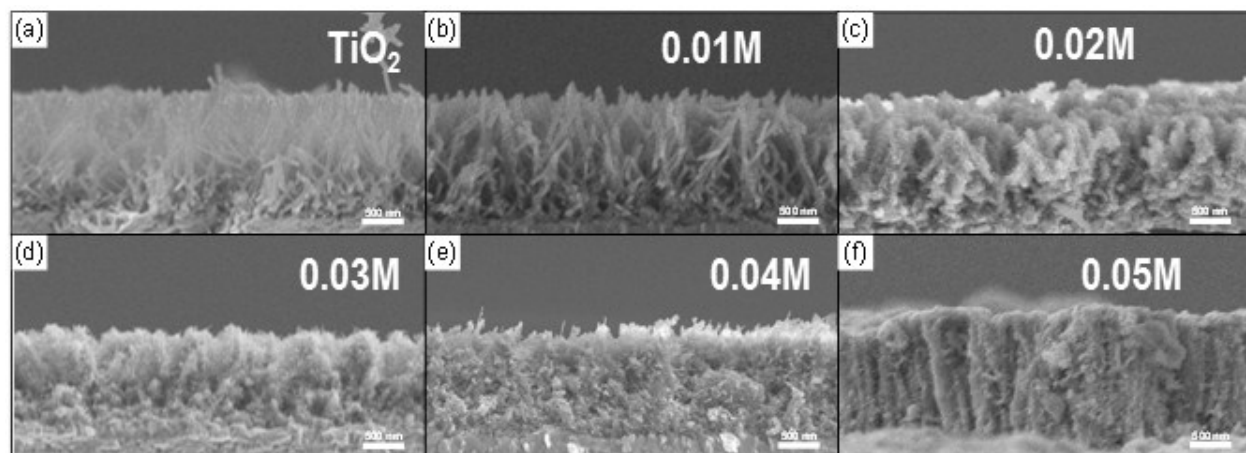


Figure S3. Cross sectional view SEM images of (a) TiO₂ NTs and (b–f) α-Fe₂O₃/TiO₂ NT composites prepared starting from Fe(III) precursor solutions with different concentrations (*i.e.*, 0.01–0.05 M).

S4. Composition analysis

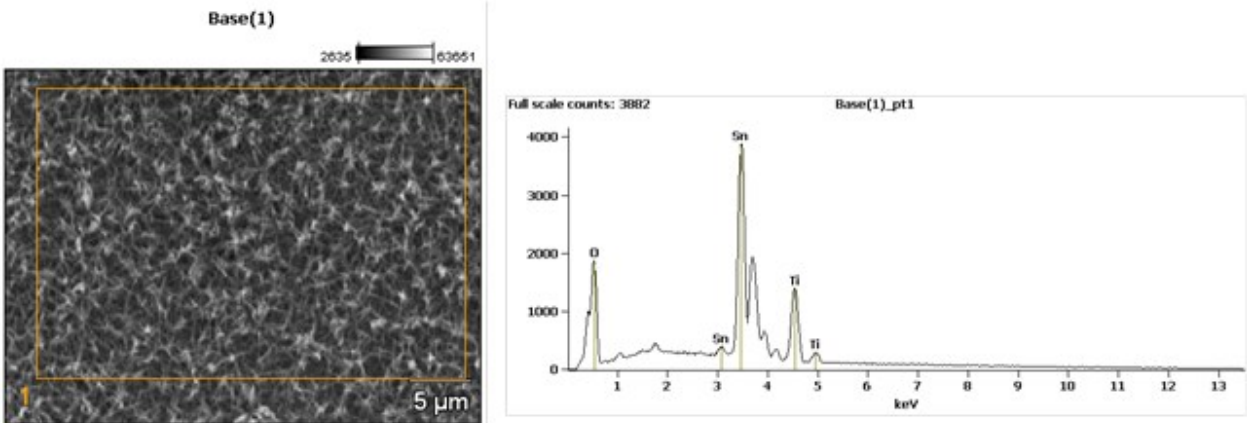


Figure S4. SEM image and corresponding EDX spectrum of pure TiO₂ NTs.

S5. Elemental mapping result

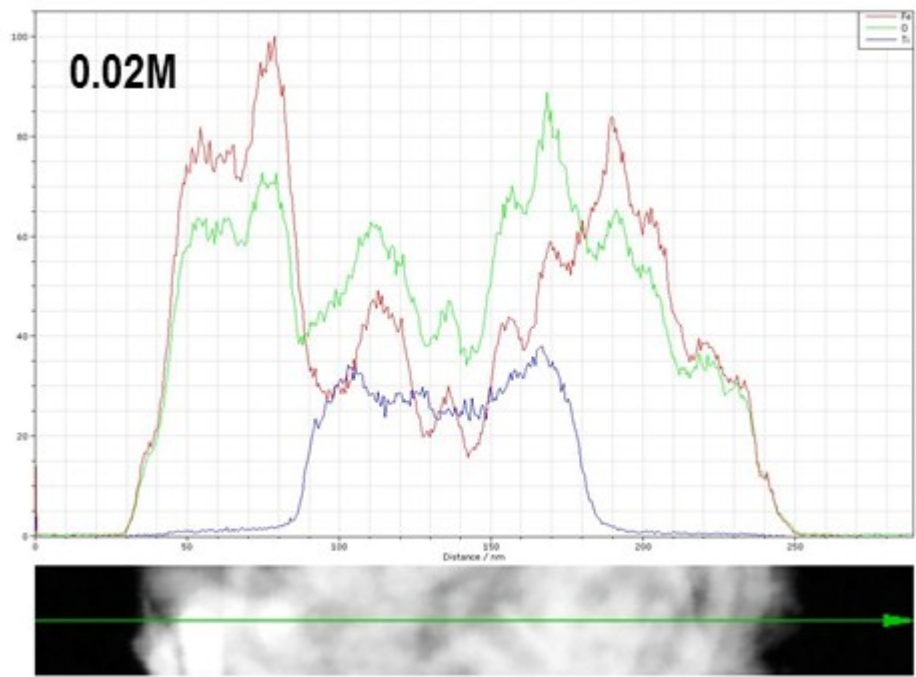


Figure S5. Auger Electron Spectroscopy (AES) horizontal mapping across the 0.02 α - $\text{Fe}_2\text{O}_3/\text{TiO}_2$ layer.

S6. Elemental mapping result

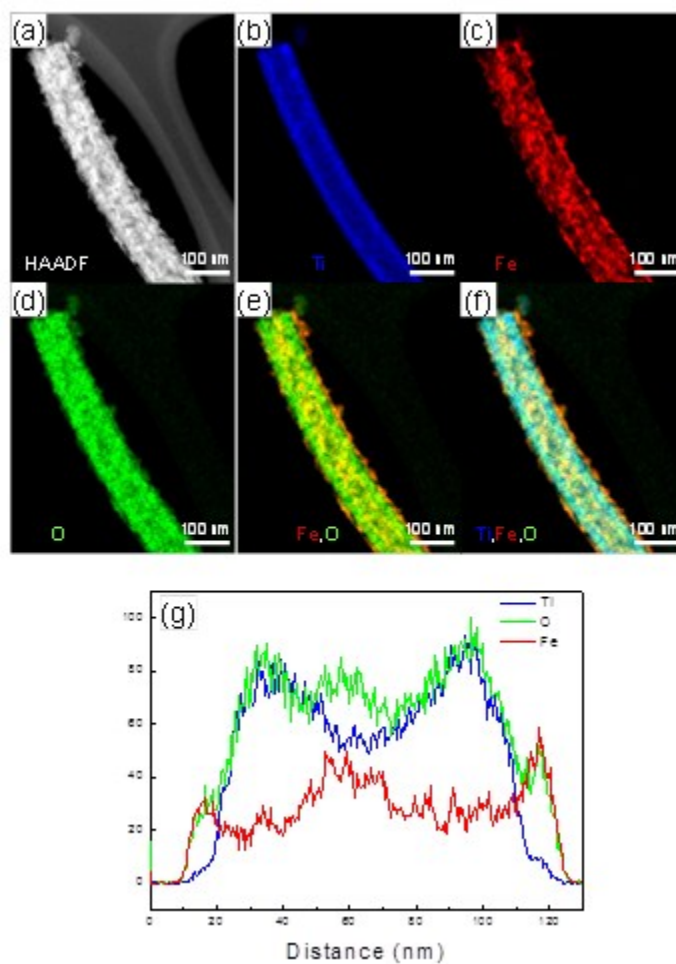
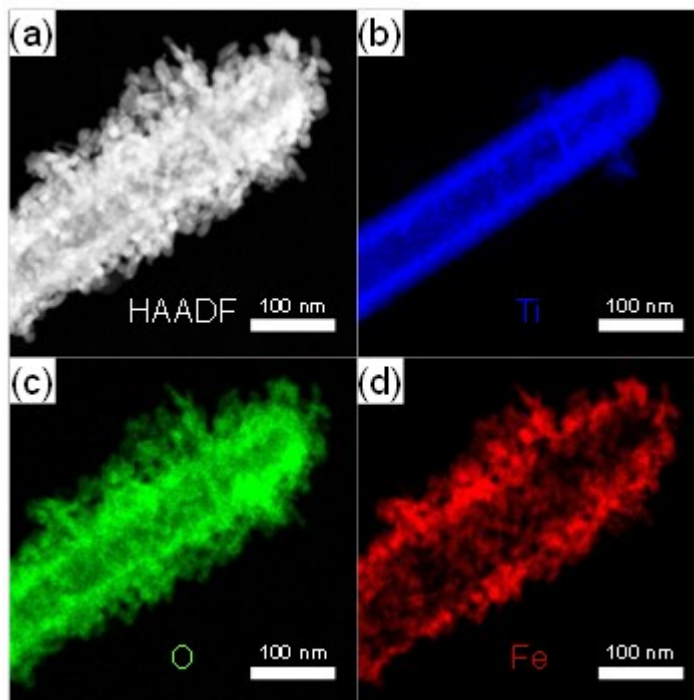


Figure S6. 0.01 α -Fe₂O₃/TiO₂ NT composite layer: (a) HAADF image and (b–f) Ti, Fe, O, Fe+O and Ti+Fe+O elemental mapping of the 0.02 Fe₂O₃/TiO₂ NT sample. (g) AES horizontal mapping.



S7. Elemental mapping result

Figure S7. 0.03 α -Fe₂O₃/TiO₂ NT composite layer: (a) HAADF and (b–d) Ti, O and Fe elemental mapping.

S8. Crystallite structure analysis

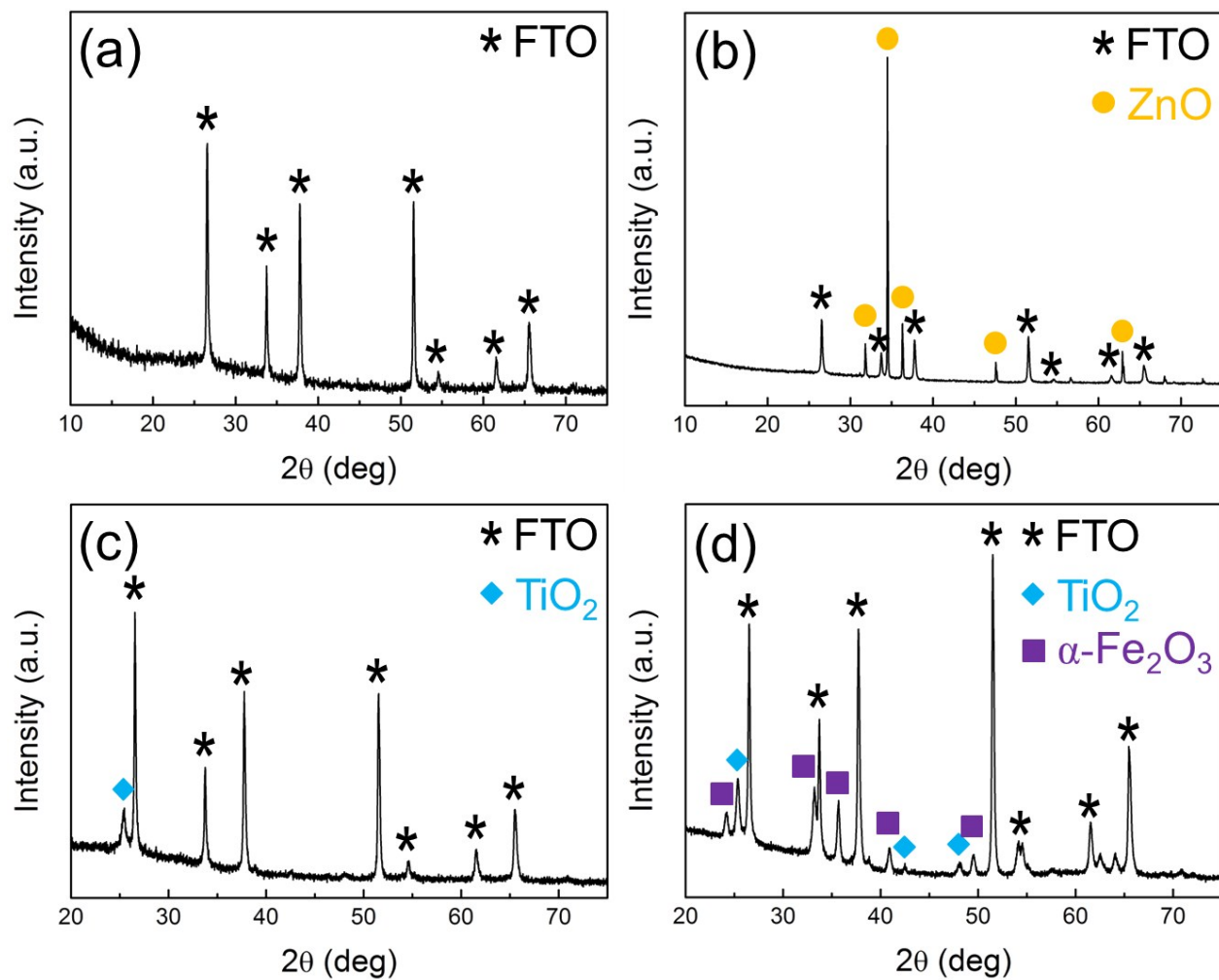


Figure S8. XRD patterns of (a) FTO layer, (b) ZnO nanorods on FTO, (c) TiO₂ nanotubes on FTO and (d) α -Fe₂O₃/TiO₂ NT composite on FTO.

S9. DFT analysis

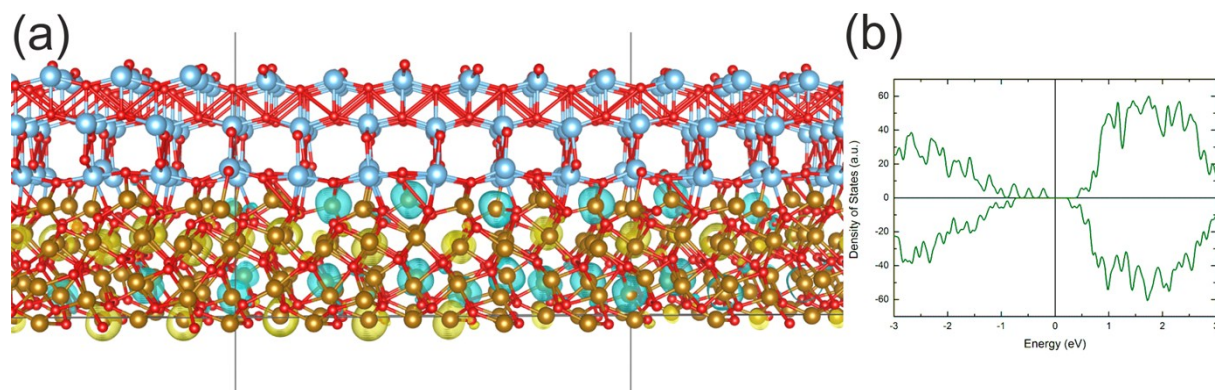


Figure S9. (a) Example of the $\alpha\text{-Fe}_2\text{O}_3/\text{TiO}_2$ heterocomposite (Ti – blue, Fe – gold, O - red) used in DFT simulations with highlighted $15.14 \text{ \AA} \times 38.04 \text{ \AA}$ computational supercell (black line) containing 81 atoms (18 Fe, 51 O, 12 Ti) and spin density (blue and yellow for up and down spin, respectively) for isovalue of 0.01 a.u. (b) Density of electronic states corresponding to the structure from (a).

S10. Steady-state photocurrent of 0.02 Fe₂O₃/TiO₂

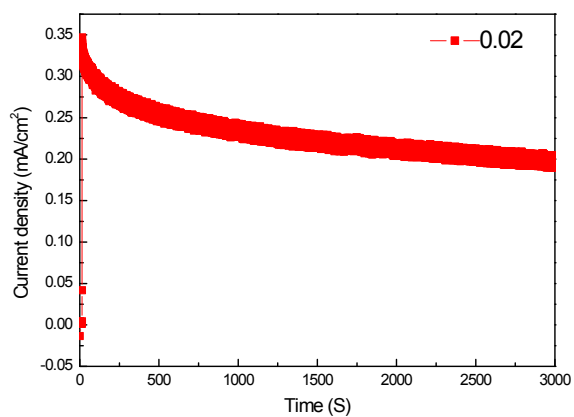


Figure S10. Steady-state photocurrent of the 0.02 Fe₂O₃/TiO₂ layer measured in 1 M NaOH at 0.8 V vs Ag/AgCl under AM 1.5G simulated sun light (100 mW cm⁻²).

S11. Photoelectrochemical water splitting with pure $\alpha\text{-Fe}_2\text{O}_3$ layers

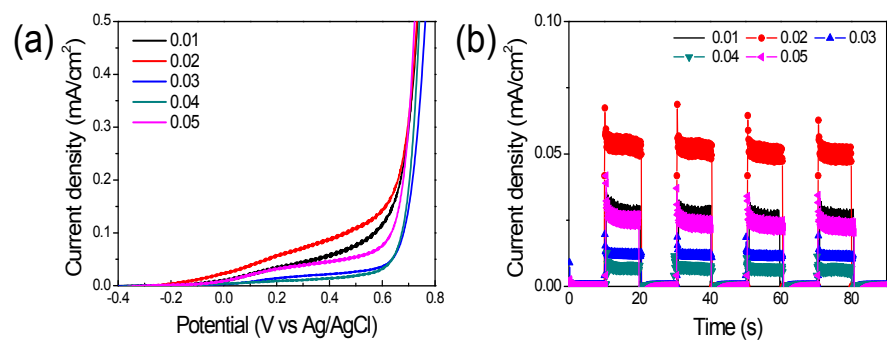


Figure S11. (a) Current-potential characteristics of $\alpha\text{-Fe}_2\text{O}_3$ on FTO, measured in 1 M NaOH at 10 mV s^{-1} scan rate, under AM 1.5G illumination. (b) Photo-transient characteristics of $\alpha\text{-Fe}_2\text{O}_3$ on FTO, measured in 1 M NaOH at $+0.26 \text{ V vs Ag/AgCl}$ and under AM 1.5G chopped light illumination.

S12. Nyquist plots of electrochemical impedance measurements of $\alpha\text{-Fe}_2\text{O}_3$ layers

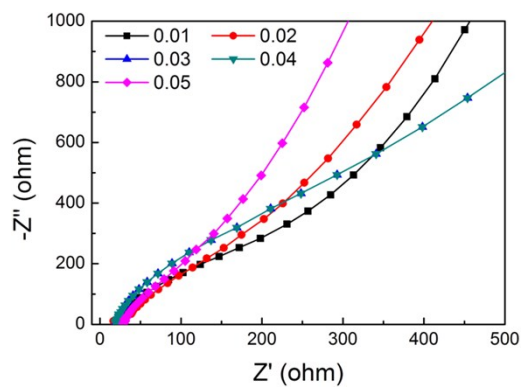


Figure S12. Nyquist plots of electrochemical impedance of $\alpha\text{-Fe}_2\text{O}_3$ on FTO, measured at +0.26 V (vs Ag/AgCl (3 M KCl)), in 1 M NaOH, under AM 1.5G illumination.